Chapter 6
Colorless Laser Diodes for DWDM-PON Transmission

Gong-Ru Lin, Yu-Chuan Su and Yu-Chieh Chi

6.1 Historical Review and Challenges on Injection-Locked Laser Diode Transmitters for DWDM-PON Transmission

6.1.1 Historical Review on the Roadmap of Injection-Locked Transmitters for DWDM-PON

Since the requirement on data transmission capacity of the broadband internet access network is persistently increasing, the remarkable efforts have been paid on both optical wavelength and electrical frequency usages of the data transmitters emerged for developing the next-generation passive optical network (NGPON). The dense-wavelength-division-multiplexed passive-optical-network (DWDM-PON) is regarded as one of the promising candidates for the fiber-to-the-home network owing to its simple architecture with extremely large transmission capacity at low cost of power budget [1, 2]. In consideration of practical optical distribution within a short-distant metropolitan network ($\leq$20 km), the wavelength injection-locked colorless laser diode is usually considered as the universal transmitter at user end due to its broadband gain-spectral range that ensures single-mode operation with enhanced modulation bandwidth at multiple DWDM channels [3, 4]. Versatile master light sources were employed to approach the injection-locking of different colorless transmitters to meet the demand of the DWDM-PON system. The historical progress and existed problem of different injection-locked transmitter with various master light sources are shown in Fig. 6.1. In 2000, Kim et al. [5] proposed an amplified spontaneous emission

G.-R. Lin (✉) · Y.-C. Su · Y.-C. Chi
Graduate Institute of Photonics and Optoelectronics, Department of Electrical Engineering, National Taiwan University, Taipei, Taiwan
e-mail: grlin@ntu.edu.tw

© Springer Science+Business Media Dordrecht 2015

C.-C. Lee (ed.), *The Current Trends of Optics and Photonics*,
Topics in Applied Physics 129, DOI 10.1007/978-94-017-9392-6_6

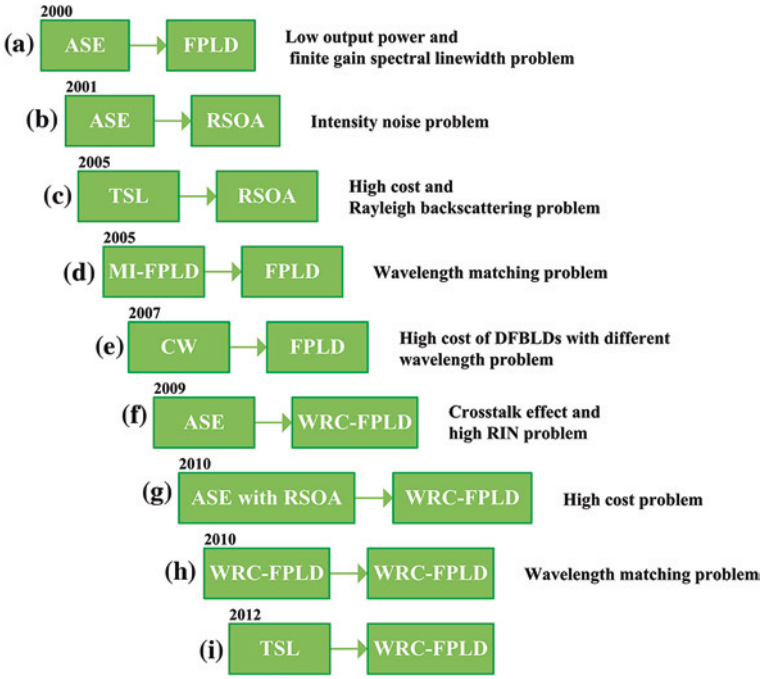

Fig. 6.1 The roadmap of DWDM-PON transmitters with external injection light source

(ASE) injection-locked Fabry-Perot laser diode (FPLD) with single-mode output as a low-cost DWDM transmitter. The side-mode suppression ratio (SMSR) and the extinction ratio (ER) of the wavelength-locked FPLD were larger than 29 and 13 dB, respectively. Owing to the high injection budget, lower output power and thermally unstable behavior, the FPLD with a finite gain spectral linewidth is hard to be externally injection-locked and thus not an ideal transmitter for broadband spectral sliced DWDM-PON system (Fig. 6.1a). Later on, the ASE injection-locked reflective semiconductor optical amplifier (RSOA) based DWDM-PON transmitter [6] was proposed to successfully provide eight DWDM channels with 1 nm wavelength spacing. With each channel modulated at a data rate of 1.25 Gbit/s, the non-return-to-zero (NRZ) on-off-keying (OOK) data transmission is shown to propagate over 25-km. However, the transmission performance is limited by the bad relative intensity noise (RIN) performance of the ASE injection source (Fig. 6.1b).

In order to reduce the ASE noise and release the limited injection-locked wavelength range, the single-mode laser (SML) injection-locked RSOA has been demonstrated. Since 2005, Lee et al. have proposed a bidirectional DWDM-PON by using a SML injection locked RSOA at gain saturation mode [7], which achieved 1.25 Gbit/s for upstream and 2.5 Gbit/s for down-stream data transmission over 20 km. Although the upstream data carried by the SML injection-locked RSOA

can be generated by remodulating the data-erased [8–10] down-stream carrier, such a down- and up-stream wavelength preserved solution is not practical for DWDM-PON due to its high cost with the need of an additional data eraser and its increasing noise caused by Rayleigh backscattering (Fig. 6.1c). In the meantime, the mutually injection-locked [11, 12] AR-coated FPLDs pair has preliminarily emerged as an alternative broadband light source (BLS) for controlling the wavelength of the slave AR-coated FPLD at user-end optical network unit (ONU) [13]. The mutually injection-locked AR-coated FPLD master exhibits a narrow channel spacing of 0.2 nm associated with an extremely low RIN, however, which requires two identical FPLDs with exactly same end-facet reflectance and cavity length to guarantee the flattened master gain spectrum with equivalent mode spacing (Fig. 6.1d). Later on, the continuous-wave (CW) injection-locked FPLD has demonstrated in 2007 [14] to solve the wavelength matching problem and provide up- and down-stream transmission up to 10 Gbit/s, due to the highly-coherent injection (Fig. 6.1e). However, the injection-locking of commercial FPLDs with high end-facet reflectance (R = 30 %) usually requires a relatively large injection level, which inevitably causes the high power budget and high equipment cost from the highly coherent single-mode master lasers. This makes the CW injection-locked FPLD less comparable with an ideal cost-effective transmitter for DWDM-PON system.

6.1.2 Development of a Promising Universal Transmitter for Colorless Operation in DWDM-PON

Recently, the AR-coated colorless FPLD with long weak-resonant-cavity (hereafter referred as WRC-FPLD) has been considered as a more potential candidate to provide dense and weak longitudinal modes for next-generation DWDM-PON system than previous works because of its broad gain-spectrum, which provides more DWDM transmission channels than common FPLD and better throughput coherence than the RSOA. The illustrated WRC-FPLD spectrum and the WRC-FPLD and traditional FPLD channelized by the 200-GHz arrayed waveguide grating (AWG) are shown in Fig. 6.2a. With the 200-GHz channel spacing, the WRC-FPLD possesses more modes in one channel than the traditional FPLD due to its smaller mode spacing. As more longitudinal modes can be modulated in one channel, the ASE injection-locked WRC-FPLD transmitter provides a better transmission performance [15]. On the other hand, the WRC-FPLD can be channelized by the AWG based multiplexer/de-multiplexer with narrower channel spacing to providing more DWDM channels in its finite gain spectrum. Figure 6.2b shows the illustrated spectrum of WRC-FPLD with ASE, WRC-FPLD and tunable single-mode laser (TSL) injection-locking. Hence, the ASE injection-locked WRC-FPLD used for DWDM-PON was proposed in previous work [15, 16], providing a bit-error-rate (BER) of 10^{-13} at receiving power of −31 dBm with a bit rate of 622 Mbit/s at least.

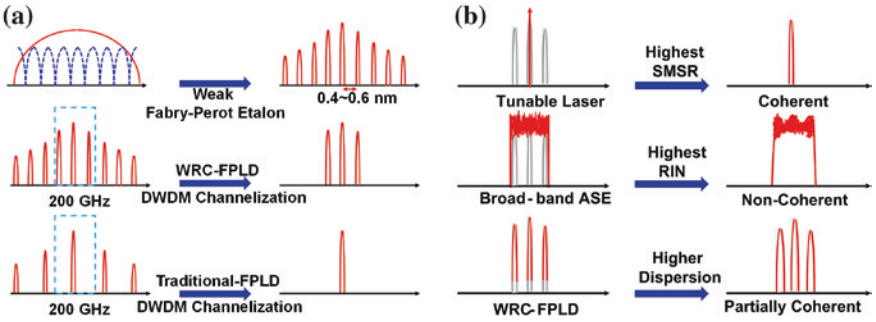

Fig. 6.2 **a** The illustrated WRC-FPLD spectrum and WRC-FPLD or traditional FPLD channelized by 200-GHz AWG. **b** Schematic of slave WRC-FPLD with TSL, ASE and master WRC-FPLD injection-locking

Owing to the fluctuant noise of the ASE source, the AWG channelized ASE injection-locked WRC-FPLD presents the highest noise, which was then considered to be reduced by changing the ASE source with the partial-coherent master WRC-FPLD. However, it is inevitable to inject-lock two or three mode within one channel when the channel spacing of AWG is not narrow enough, which may result in the unexpected dispersion during long-distant transmission. This dispersion effect can be solved by using the dispersion compensation fiber (DCF) [16] but is not practical for the existing long-haul fiber network. Another solution is the use of the TSL to injection-lock WRC-FPLD, which shows a perfectly single-mode output with the highest SNR, narrowest linewidth and lowest dispersion to provide a better transmission quality. When comparing the conventional FPLD (front facet reflectance of 30 %) with the WRC-FPLD (front facet reflectance of 1 %) [17], the WRC-FPLD possess the higher SMSR at the same injection power level and the wider detuning of injection-locked wavelength [18] than the traditional FPLD [19] owing to its weak-resonant-cavity feature.

To effectively increase the network capacity of the DWDM-PON system with the injection-locked WRC-FPLD transmitter, both the 200-GHz and the 50-GHz AWG were considered to slice the ASE injection source with their chirp, noise and transmission performances compared each other [20]. Although the DWDM-PON system with 50-GHz AWG can provide more channels with lower negative frequency chirp than those with the 200-GHz AWG, the 200-GHz AWG channelized ASE injection minimizes the intensity noise of WRC-FPLD transmitter to perform better transmission performance. With the additional AWG filtering, the RIN induced by ASE source and the intraband crosstalk [21] between the upstream transmitted data and the reflected ASE signal are two important issues of the DWDM-PON system with the ASE injection-locked WRC-FPLD transmitter. A solution has been proposed in previous work by using the SOA based noise reduction [22] to squeeze the ASE noise at local ONU part to solve

these problems, and the RIN and the crosstalk effect can be reduced by 4.5 and 6.3 dB, respectively [23]. Although the noise of the ASE injection source could be minimized by the saturable RSOA, the extra RSOA in each ONU channel inevitably raises the cost for the DWDM-PON system. After considering the noise and cost of the ASE injection-locked WRC-FPLD applied to the DWDM-PON system, the mutually injection-locked FPLD [24] was proposed to meet these demands. Afterwards, the partially coherent WRC-FPLD injection-locked WRC-FPLD has also emerged [25], which shows an SMSR of up to 40 dB and a Q factor of 9.5 dB to provide a receiving sensitivity of −24.4 dBm at a BER of 10^{-12} in the 2.5-Gbit/s DWDM-PON transmission. More recently, the highly coherent tunable CW fiber laser was employed to solve the wavelength matching problem between the master and slave lasers [26]. Particularly, the transmission performance of the injection-locked WRC-FPLD transmitters with different front-facet reflectances were also investigated [27]. In contrast to the WRC-FPLD injection-locked WRC-FPLD, the TSL injection-locked WRC-FPLD has also been proposed, as shown in Fig. 6.1h, which offers the highest SNR to obtain the ultimate transmission performance when comparing with the ASE and the WRC-FPLD injection-locking cases.

6.1.3 Using Long-Cavity Colorless Laser Diodes for OOK/OFDM Transmission in DWDM-PON

When considering the back-to-back and 25-km single-mode fiber (SMF) transmissions, the measured eye-diagrams of the free-running and ASE injection-locked WRC-FPLDs under direct on-off keying (OOK) modulation are compared in Fig. 6.3. The back-to-back transmitted eye-diagram of WRC-FPLD without injection-locking is clearer than that of the ASE injection-locked WRC-FPLD, since all longitudinal modes of the free-running WRC-FPLD under direct modulation are received without spectral slicing. However, the eye-diagram of the free-running WRC-FPLD is seriously distorted after 25-km SMF transmission because these longitudinal modes covering a broadband gain spectrum results in strong modal dispersion after long-distant transmission. In contrast, the single-mode injection-locked WRC-FPLD exhibits a narrower linewidth to minimize the dispersion effect and provide a clearer eye-diagram after the 25-km transmission. For increasing the transmission data rate, it is necessary to enhance the modulation bandwidth of such a broadband WRC-FPLD transmitter by enlarging its bias current or injection-locking power. An alternative approach of carrying the high capacity data in finite bandwidth can be achieved by using the orthogonal frequency-division multiplexing (OFDM) modulation format [28, 29]. Transmission of the OFDM data were successively demonstrated with the distributed feedback laser diodes (DFBLDs) [30, 31], the vertical-cavity surface emitting laser diodes (VCSELDs) [32, 33], the TSL injection-locked WRC-FPLD [34] and the down-stream reusable RSOA [35, 36]. The OFDM

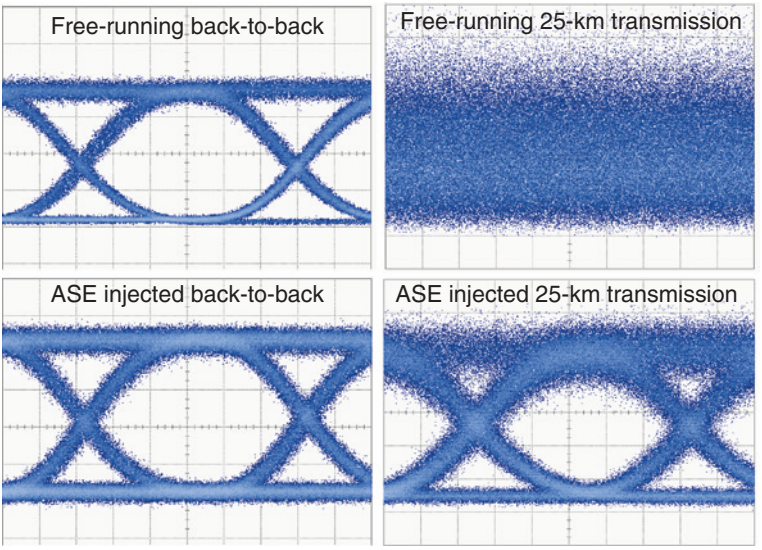

Fig. 6.3 The measured back-to-back and 25-km transmitted eye-diagrams of the WRC-FPLDs without and with spectrum-sliced ASE injection

modulated WRC-FPLD or RSOA transmitter provides the high spectral usage to achieve the data rate of 4 or 7.5–10 Gbit/s by efficiently using the modulation bandwidth of only 1 GHz. Not long ago, the TSL injection-locked WRC-FPLD with the data transmission rate up to 20 Gbit/s by pre-leveling technique was reported [37]. It is known that the OFDM modulation format consisted of intensity and phase signals is sensitive to the coherence of transmitters; however, the comparisons on the OFDM performance of the WRC-FPLD transmitters injection-locked by master sources with different degrees of coherence have never been discussed.

Although the laser throughput properties and transmission performance can be improved by enhancing the coherence of injection light source, higher coherent injection light also inevitably raises the equipment cost. In this work, the effect of injection coherence on the noise, bandwidth and error rate performances of the long-cavity colorless WRC-FPLD with an end-facet reflectance of 0.5 % is demonstrated for OOK and OFDM transmission. By using three kinds of master sources with different degrees of coherence including an AWG channelized ASE, free-running WRC-FPLD and TSL, several key parameters of the wavelength injection-locked slave WRC-FPLD transmitter such as the RIN, the frequency response, the signals to noise ratio (SNR) and the bit error rate (BER) of OOK and 16-QAM OFDM transmitted data are characterized. In addition to the throughput response and transmission performance, the simulated eye diagrams from a set of modified rate equations are compared with the experimental results.

6.2 OOK or OFDM Data Transmission Performances of Directly Modulated Slave WRC-FPLD Injection-Locked by Master Sources with Different Degrees of Coherence

6.2.1 Methods for Building up the DWDM-PON with Directly Modulated Slave WRC-FPLD Injection-Locked by Master Sources with Different Degrees of Coherence

The Fig. 6.4 illustrates a DWDM-PON system based on the up-stream WRC-FPLD transmitter with a front-facet reflectance of 0.5 %. The slave WRC-FPLD is injection-locked by the channelized ASE light source, master WRC-FPLD or tunable laser (Agilent, 8164A) in the central office, respectively. The external injection-locking was performed by seeding the non-coherent, partial coherent or high coherent light sources with fixed output power of −6 dBm into the WRC-FPLD through a polarization controller, and passing through a 100-GHz AWG multiplexer.

In the transmission part of the ONU, the DC bias current and the modulation signal with OOK or OFDM modulation format was coupled into a bias-tee (Mini-circuits, ZX85-12G-S+) for driving the WRC-FPLD. The bias current of WRC-FPLD directly modulated by a 1.25-Gbit/s OOK data-stream with a pattern length of $2^{23} - 1$ was set nearby 34 mA corresponding to 2 I_{th} to achieve the optimized ER for transmission diagnosis. The peak-to-peak amplitude of the electrical PRBS digital data was set at 500 mV. In the receiver part of the ONU, the eye-diagram and BER of the slave WRC-FPLD based up-stream transmitted data was analyzed by a digital sampling oscilloscope (Agilent, 86100A + 86109B) and commercial error detector (Agilent, 70843A). The OFDM signal was sent to an arbitrary waveform generator (Tektronix 7102B) with a central frequency at 1.5625 GHz, a carrier number of 122, a sampling rate of 12.5 GHz, a total bit rate at 12.5 Gbit/s and

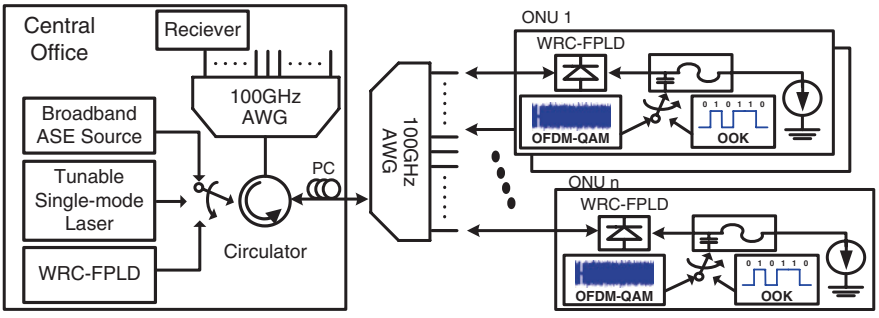

Fig. 6.4 A DWDM-PON system with a coherent laser, WRC-FPLD or ASE injection-locking source located at central office

a modulation bandwidth of 3.125 GHz. The transmitted OFDM signal delivered by the slave WRC-FPLD injection-locked with different master sources were analyzed by a real-time digitized oscilloscope analyzer (Tektronix CSA7404B) with a sampling rate of 100 GS/s.

6.2.2 *The Effect of the Injection Coherence on Mode, Noise Characteristics and Frequency Response*

The full-band spectra of the WRC-FPLD at free-running condition or under injection-locked by using non-coherent ASE, partially coherent WRC-FPLD and highly coherent TSL are compared in the upper row of Fig. 6.5. The free-running WRC-FPLD exhibits an extremely wide gain spectrum with numerous weak-resonant longitudinal modes covering the wavelength from 1,530 to 1,585 nm. Such a broad lasing spectrum of the WRC-FPLD is comparable with the gain spectrum of a free-running SOA, indicating that the extremely weak Fabry-Perot etalon effect is introduced by the relatively small end-facet reflectance of 0.5 %. With same injection level of −6 dBm, all the injection-locked spectra reveal single mode operation. However, the zoom-in lasing spectra (see middle row of Fig. 6.5) of the single-mode WRC-FPLD injection-locked by three master sources with different degrees of coherence can still be distinguished from one another. After injection-locking with the broad-band ASE source channelized by using an AWG

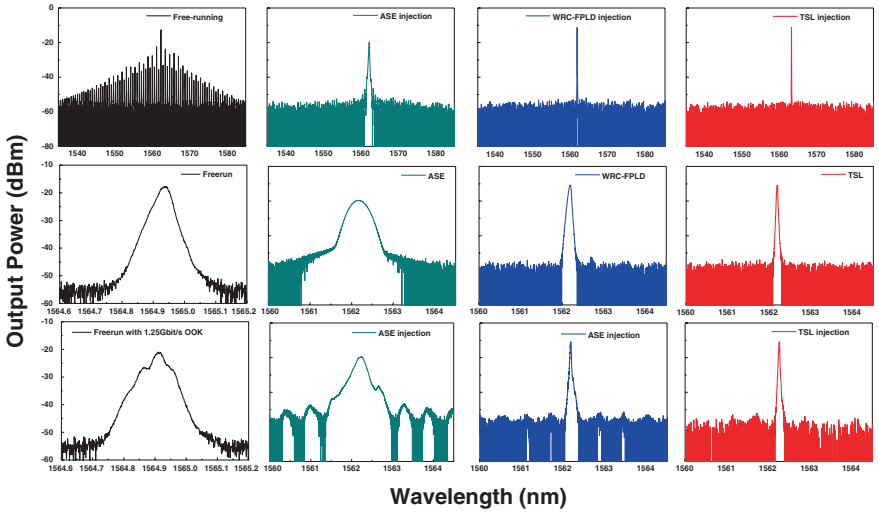

Fig. 6.5 The continuous-wave operated (*upper* for full-band and *middle* for zoom-in spectra) and the OOK modulated (*lower*) optical spectra of the slave WRC-FPLDs under free-running (*first column*) and injection-locked with non-coherent ASE (*second column*), partially coherent WRC-FPLD (*third column*) and highly coherent TSL (*forth column*)

demultiplexer with a channel spacing of 100 GHz (0.8 nm), the slave WRC-FPLD presents a much broader mode linewidth of up to 0.724 nm. In contrast, the WRC-FPLD injection-locked WRC-FPLD pair results in a mode linewidth as narrow as 0.146 nm. In comparison with those master sources with lower coherence, the highly coherent TSL consists of more coherent photons at a cavity resonant wavelength to shrink the slave WRC-FPLD linewidth to 0.086 nm and suppress its relative intensity noise. Owing to the higher coherence and lower ASE noise of TSL, the TSL injection-locked WRC-FPLD presents a narrowest mode spectrum.

After 1.25 Gbit/s OOK modulation, the OOK modulated modal linewidths of the WRC-FPLD injection-locked by 100-GHz AWG channelized ASE, master WRC-FPLD and TSL are 0.8, 0.21 and 0.09 nm respectively (see the lower row of Fig. 6.5). Because the 100-GHz AWG channel spacing (0.8 nm) is much broader than the mode spacing (0.5 nm) of the WRC-FPLD, the adjacent side-modes near by the major injection-locked mode of the WRC-FPLD are inevitably injected by channelized ASE slightly. The inevitably injected side-modes and broader linewidth of laser transmitter are not beneficial for long-distance transmission due to the mode-beating and dispersion effects. Technically, the adjacent side-modes of the slave WRC-FPLD injection-locked by the ASE and the master WRC-FPLD can be filtered out by using an AWG demultiplexer with channel spacing of 50 GHz in DWDM-PON. However, the AWG channelized ASE injection-locked WRCFPLD also degrades its transmission performance when narrowing down the AWG bandwidth as which inevitably increases the intensity noise [20]. In comparison with the ASE injection-locking case, the master WRC-FPLD and TSL not only suppress the side-modes of the slave WRC-FPLD but also lead to a narrower linewidth. With the same injection power, the side-mode suppression ratios (SMSRs) of WRC-FPLD injection-locked by ASE, master WRC-FPLD and TSL are 27, 40.5 and 45.3 dB, respectively.

Besides, the wavelength tunability of the master WRC-FPLD and TSL enables the exact wavelength coincidence with the slave WRC-FPLD. The injection master with higher coherence ensures more stimulated emitting photons created in the injection-locked mode, which provides the slave WRC-FPLD transmitter better coherent throughout and higher SMSR. Undoubtedly, the non-coherent ASE master consists of large intensity and phase noise, and the phase noise also cross-correlates with the intensity noise through the rate equations [38]. Improving the master coherence effectively reduces both phase and intensity fluctuations due to the enhanced stimulated emission. As evidence, the RIN spectra of master ASE, WRC-FPLD and TSL at constant power of −6 dBm after passing through the 100-GHz channelized AWG are shown in Fig. 6.6. The non-coherent ASE shows the RIN floor as high as −95 dBc/Hz, which is 5–12 dB worse than the WRC-FPLD and TSL masters. The WRC-FPLD master exhibits comparable RIN with the TSL at frequency higher 5 GHz, whereas its low-frequency RIN level is degraded by 5 dB with frequency decreasing from 5 to 1 GHz. After injection-locking by masters with different degrees of coherence, the RIN spectra of slave WRC-FPLDs under injection-locking powers of −12 and −6 dBm are compared in Fig. 6.7.

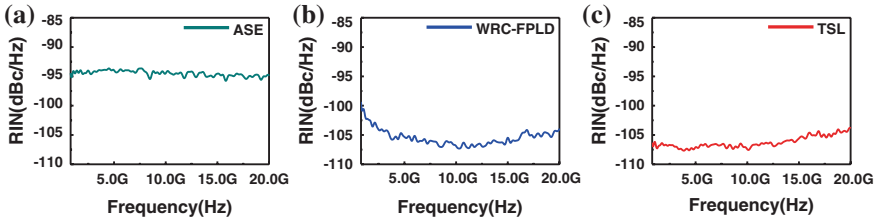

Fig. 6.6 The RIN spectra of master ASE, WRC-FPLD and TSL after the 100-GHz AWG

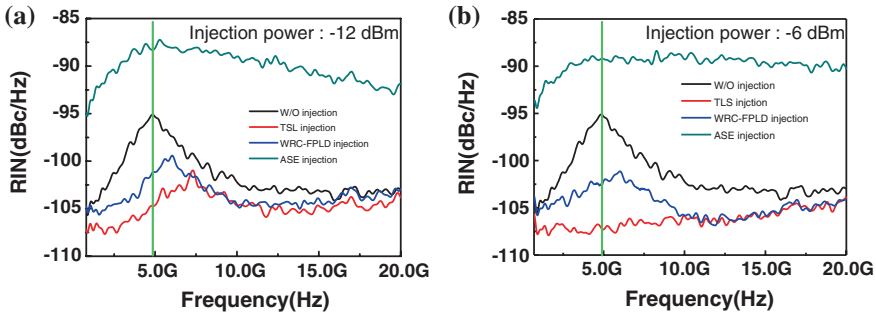

Fig. 6.7 The RIN of slave WRC-FPLD injection-locked by TSL, WRC-FPLD and ASE at injection powers of **a** −12 dBm and **b** −6 dBm

The free-running WRC-FPLD reveals a relaxation oscillation peak with intensity of −95 dBc/Hz at 5 GHz. Improving the coherence of master not only suppresses the RIN floor but also shift the relaxation oscillation peak of slave WRC-FPLD under injection-locking. The ASE injection-locking fails to improve the RIN of the slave WRC-FPLD. At −12 dBm injection, the slave WRC-FPLD shows a RIN peak that is 7 dB larger than that of the original ASE master. The non-coherent injection greatly degrades the RIN by raising its floor up to 10 dB, which cannot be improved simply by enlarging the injection-locking power, as shown in Fig. 6.7b. In contrast, the injection of a partially coherent WRC-FPLD master slightly up-shift the RIN peak to 6 GHz and reduces its intensity by 10–15 dB as compared to the ASE injection-locking case. The 6-dB increment on the injection level could further reduce the entire noise background linearly. Both the WRC-FPLD and TSL maters improve the RIN of the slave WRC-FPLD; however, the TSL shows a superior capability on suppressing the RIN background at smaller frequencies. Furthermore, the relaxation oscillation peak up-shifts and even disappears with enlarging injection level. Such a lowest RIN floor explains why the highly coherent TSL inject-locked WRC-FPLD exhibits the highest SMSR.

Subsequently, the analog modulation response of the slave WRC-FPLD injection-locked by different masters with injection powers of −12 and −6 dBm are compared in Fig. 6.8a, b. With injection-locking, the modulation response in

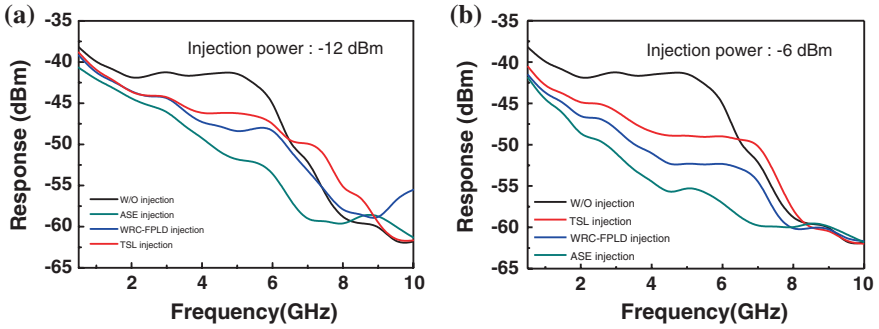

Fig. 6.8 The frequency response of slave WRC-FPLD injection-locked by TSL, WRC-FPLD and ASE at injection powers of **a** −12 dBm and **b** −6 dBm

high-frequency region can be enhanced at a cost of sacrificing the throughput power in low-frequency region. The enhanced coherence of master simultaneously suppresses the RIN floor and improves the modulation bandwidth with up-shifted relaxation oscillation frequency. The ASE injection-locked WRC-FPLD shows lowest modulation throughput with its power-to-frequency slope increasing from −2.2 to −3.4 dB/GHz by enlarging the injection from −12 to −6 dBm. The injection-locked master-slave WRC-FPLD pair performs an increment on the relaxation oscillation frequency from 5 GHz (free-running case) to 6–6.5 GHz; however, the enlarged injection power from −12 to −6 dBm pays more the throughput power attenuation than the frequency bandwidth extension. The highly coherent TSL injection-locks the slave WRC-FPLD and further up-shifts its relaxation oscillation frequency from 5 to 7 GHz. In comparison, the slave WRC-FPLD exhibits a larger throughput at lower injection level, and a trade-off is set between injection level and modulation bandwidth.

6.2.3 The Effect of Injection Coherence on OOK Transmission Performances of the Slave WRC-FPLD Laser Transmitter with Different-Locking Master Sources

The measured and simulated eye-diagrams of the directly modulated and AWG channelized WRC-FPLD injection-locked by versatile light sources with different degrees of coherence are compared in Fig. 6.9a, b. When comparing with other two cases, the measured eye-diagrams of the ASE injection-locked WRC-FPLD shows an ER of 8.02 dB and a relatively low SNR of 6.07 dB owing to its intense noise at on-level. That is, the ASE process continues in the slave WRC-FPLD to cause more non-coherent photons with randomized phases. Increasing the degree of coherence by changing the master from ASE to WRC-FPLD could effectively

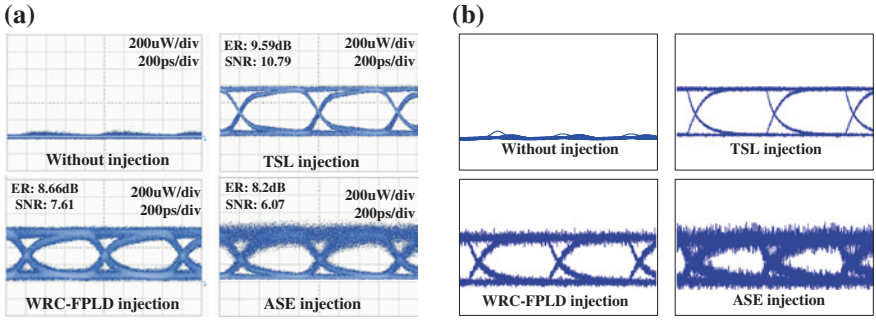

Fig. 6.9 **a** The measured and **b** the simulated eye-diagrams of WRC-FPLDs without and with TSL, WRC-FPLD and ASE injection

improve the SNR of the slave WRC-FPLD transmitted data from 6.07 to 7.61 dB at same power level. Obviously, the TSL injection-locked WRC-FPLD shows greatly optimized ER of 9.6 dB and SNR of 10.8 dB with a injection-locking level of −3 dBm. Note that the increment of ER is attributed to the noise suppression of off-level data, and the enhancement on SNR is owing to the reduction of the RIN at on-level. Increasing the coherence of injection-locking master effectively contributes to a significant suppression on the on- and off-level noises such that the better enhancement of both the SNR and the ER can be achieved.

In simulation, the following rate equations adopting by the theoretical model of a single-wavelength FPLD [38] under external injection-locking condition are shown below,

$$\frac{dN(t)}{dt} = \frac{\eta_i I}{qV} - \frac{N(t)}{\tau_s} - \frac{v_g a}{V}[N(t) - N_{tr}]S(t), \tag{6.1}$$

$$\frac{d\phi(t)}{dt} = \frac{\alpha}{2}\{\frac{\Gamma v_g a}{V}[N(t) - N_{tr}] - \frac{1}{\tau_p}\} - \kappa\sqrt{\frac{S_{inj} + \Delta S \cdot Rand(t)}{S(t)}}\sin\phi(t) - \Delta w_{inj}, \tag{6.2}$$

$$\frac{dS(t)}{dt} = \frac{1}{2}\{\frac{\Gamma v_g a}{V}[N(t) - N_{tr}] - \frac{1}{\tau_p}\}S(t) + \kappa\sqrt{[S_{inj} + \Delta S \cdot Rand(t)]S(t)}\cos(\phi(t)), \tag{6.3}$$

where $N(t)$, $\Phi(t)$ and $S(t)$ are the time dependent functions of carrier number, phase and photon number of the slave WRC-FPLD, respectively. In these equations, I denotes the biased current, η_i the internal quantum efficiency, a the differential gain, Γ the optical confinement factor, v_g the velocity, τ_p the photon lifetime, τ_s the spontaneous carrier lifetime, κ the coupling efficiency, α the linewidth enhancement factor, S_{inj} the injection photon and $\Delta\omega_{inj}$ the detuning frequency.

To present all simulated eye-diagrams of the WRC-FPLD injection-locked by master sources of different degrees of coherence, the related parameters are

Table 6.1 The parameters of the WRC-FPLD injection-locked by master sources of different degrees of coherence

Master sources	ASE	WRC-FPLD	TSL
The percentage of non-coherent photons (%)	60	40	<10
Active layer thickness (μm)	0.081		
Cavity length (μm)	681		
Active layer width (μm)	1.5		
Rear facet reflectance	93 %		
Front facet reflectance	0.5 %		
Carrier number at transparency	8.27E7		
Carrier number at threshold	1.67E8		
Carrier lifetime (ns)	1.00		
Photon lifetime (ps)	1.39		
Optical confinement factor	0.23		
Mirror loss (cm^{-1})	78.75		
Threshold gain (cm^{-1})	364.14		
Group velocity (cm/s)	8.57E9		

summarized in Table 6.1. The degrees of injection coherence indicate the phase consistency of photons in WRC-FPLD, which directly induces the noise fluctuation through the phase-intensity conversion in the WRC-FPLD or after passing through dispersion material such as optical fiber. In approximation, the degree of coherence can be approached by changing the weighting factor of randomized intensity term from master source. During simulation, the injection light with different coherences is approached by substituting the S_{inj} into the $S_{inj} + \Delta S \cdot Rand(t)$, where $Rand(t)$ is a random function presenting the noise fluctuation, ΔS the percentage of the non-coherent photon number. As expected, the decreased coherence of injection also increases the fluctuation of stimulated emitting photon number as well as the intensity noise in slave WRC-FPLD cavity, as shown in Fig. 6.9(b). The eye-pattern of the free-running WRC-FPLD is hardly recognized due to the spreading modulation power over all longitudinal modes of the WRC-FPLD. Nevertheless, the eye-diagrams can be significantly improved by implementing the injection-locking with enhanced coherence.

With the definition of $Q = [(ER\text{-}1)/(ER + 1)](M \bullet SNR)^{0.5}$ (which decides the lowest BER in a DWDM-PON with an optical receiver gain of M). The least Q factor to perform error-free transmission at BER < 10^{-9} is 6, and the ASE injection-locked WRC-FPLD with degraded ER and SNR shows a smallest Q of 6.2. The slave WRC-FPLD can enhance its Q factor from 6.95 to 8.5 by changing the master from partially coherent WRC-FPLD to highly coherent TSL. Under back-to-back transmission at bit rates of 1.25 and 2.5 Gbit/s, the BER responses of the slave WRC-FPLD injection-locked with different masters are compared in Fig. 6.10. Non-coherent ASE injection-locked WRC-FPLD causes a large amount of the transmission errors to limit its minimal BER of 10^{-9} at a receiving power of 21.8 dBm. The partially coherent WRC-FPLD injection achieves better ER and

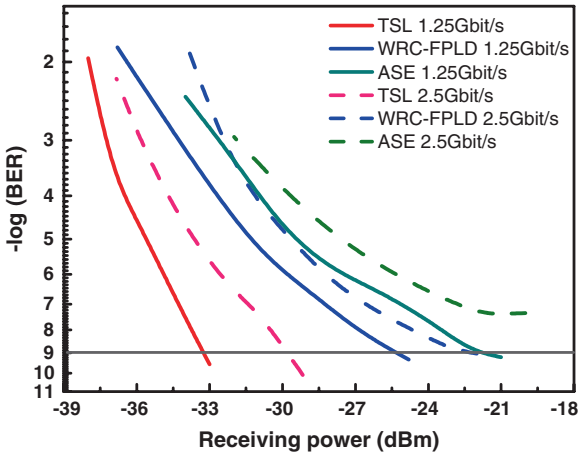

Fig. 6.10 BER of ASE, WRC-FPLD and TSL injection-locked WRC-FPLDs

SNR, thus providing a receiving power as low as −25.5 dBm for BER of 10^{-9}. The WRC-FPLD injection-locked by a highly coherent TSL greatly promotes its receiving sensitivity to −33 dBm at a BER of 10^{-9}. When comparing the 1.25- and 2.5-Gbit/s transmissions carried by the slave WRC-FPLD injection-locked with masters of different coherences, the receiving power penalty of 2–3 dB is observed by upgrading the bit rates from 1.25 to 2.5 Gbit/s. The ASE injection-locked WRC-FPLD transmitter at a bit rate of 2.5 Gbit/s shows a BER floor at around 3×10^{-7} even with the receiving power enlarging up to −20.5 dBm.

On the other hand, the performances of 16-QAM OFDM carried by using the slave WRC-FPLD injection-locked with different masters are compared with their transmitted data-stream in time and frequency domains shown in Figs. 6.11 and 6.12. In contrast to the electrical 16-QAM OFDM shown in Fig. 6.11a with a sampling rate of 12.5 GS/s, the ASE injection-locked WRC-FPLD delivers a distorted and noisy OFDM waveform with its cyclic prefix and training symbol lost during transmission (see Fig. 6.10b). The OFDM signal carried by the master WRC-FPLD injection-locked WRC-FPLD shows smaller peak-to-peak amplitude with clearer cyclic-prefix and training symbol (Fig. 6.11c), which is correlated with its broadened modal linewidth with larger intensity noise at lower frequency region. When injection-locked by partially coherent WRC-FPLD or non-coherent ASE, a nonlinearly distorted OFDM trace in time domain may by induced by modulation distortion and frequency chirp of the slave WRC-FPLD with a wider modal linewidth [16]. The completely non-distorted OFDM waveform carried by directly modulated WRC-FPLD is received when injection-locking by the highly coherent TSL master.

Since OFDM utilizes multiple subcarriers to encode the digital data-stream in parallel, the SNR feature at all subcarriers plays an important role on the overall OFDM transmission performance. From the OFDM spectrum in frequency

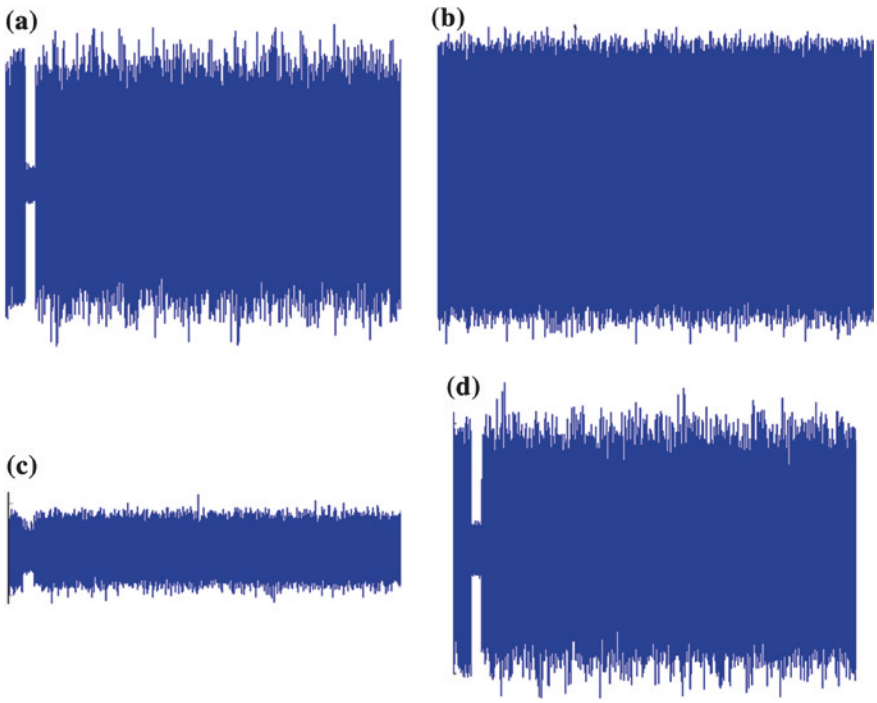

Fig. 6.11 Time-domain waveforms of 16-QAM OFDM data-streams carried by lave WRC-FPLD injection-locked by different masters. **a** Electrical waveform. **b** ASE. **c** WRC-FPLD. **d** TSL

domain shown in Fig. 6.12, the OFDM data-stream carried by ASE injection-locked WRC-FPLD reveals a totally reshaped and didtorted spectrum dominated by RIN. The whole data carried by both low- and high-OFDM subcarriers are covered with RIN and the ASE carrier is too noisy to provide high-SNR OFDM transmission, as shown in Fig. 6.12b. Owing to its lowest frequency response as well as the highest RIN, the received OFDM spectrum from the ASE injection-locked WRC-FPLD is similar to the RIN performance of the ASE injection source shown in Fig. 6.7a. In contrast, the master WRC-FPLD injection-locked WRC-FPLD scales down its noise floor with the greatly suppressed RIN (see Fig. 6.12c); however, the lower OFDM spectral power is observed due to its low modulation throughout. With the modulation response improved by highly coherent TSL injection-locking, the 16-QAM OFDM data-stream can be correctly analyzed with lowest noise floor as well as distinguished SNR at high subcarriers, as shown in Fig. 6.12d.

The constellation plots of the decoded 16-QAM OFDM data also present different degrees of amplitude and phase errors by injection-locking the WRC-FPLD with masters of different coherences, as shown in Fig. 6.13. The phase noise is mainly attributed to the frequency chirp affected by the modal linewidth of the

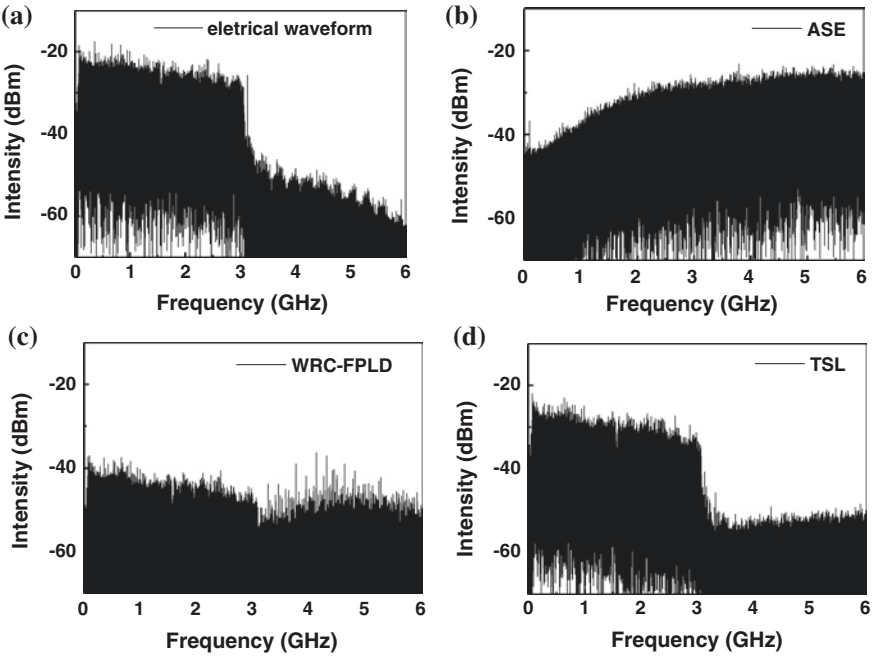

Fig. 6.12 RF spectra of 16-QAM-OFDM data-streams carried by lave WRC-FPLD injection-locked by different masters. **a** Electrical waveform. **b** ASE. **c** WRC-FPLD. **d** TSL

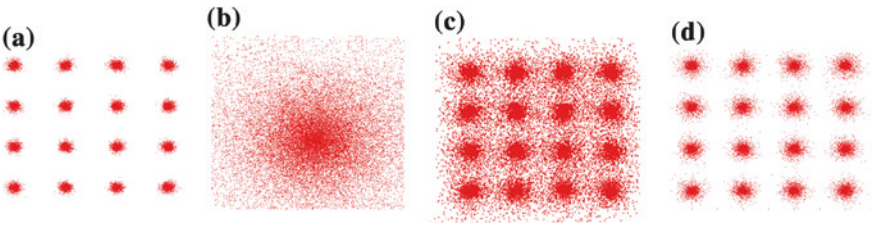

Fig. 6.13 The constellation plots of up-stream 16-QAM OFDM data-streams carried by the slave WRC-FPLD injection-locked with ASE, WRC-FPLD and TSL masters. **a** Electrical waveform. **b** ASE. **c** WRC-FPLD. **d** TSL

injection-locked slave WRC-FPLD, whereas the amplitude error results from the clamped OFDM output with limited modulation response of the WRC-FPLD. In Fig. 6.12b, the ASE injection-locked WRC-FPLD with largest RIN and lowest bandwidth fails to demonstrate a clear constellation plot, leading to an extremely large EVM as compared to its original value of 2 % (see Fig. 6.12a). The master WRC-FPLD injection-locked WRC-FPLD performs a resolvable constellation plot with an EVM of 6.9 %, as depicted in Fig. 6.12c. The clearest constellation plot of the 16-QAM OFDM data carried by the highly coherent TSL injection-locked

Table 6.2 BER and SNR of 16-QAM OFDM signals transmission with TSL, WRC-FPLD and ASE injection

Source	TSL	WRC-FPLD	ASE
Coherence	Complete	Partial	None
EVM (%)	4.5	6.9	≫20
SNR (dB)	22.8	14.7	10.2
BER	4.38E-09	5.90E-03	1.50E-01

WRC-FPLD with a minimized EVM of 4.5 % is obtained and shown in Fig. 6.12d. In summary, the EVM, SNR and BER of the decoded OFDM data carried by the slave WRC-FPLD injection-locked with masters of different coherences are listed in Table 6.2.

Obviously, the ASE injection-locked WRC-FPLD shows the worst BER response for both OOK and OFDM transmissions because the disordered OFDM waveform experiences finite modulation response with enormous noise. The master WRC-FPLD injection-locked slave WRC-FPLD can transmit the 16-QAM OFDM data-stream with a acceptable BER of 5.9×10^{-3}. The best OFDM transmission is obtained with the TSL injection-locked WRC-FPLD, which presents the narrowest mode with lowest noise to carry the OFDM data with a receiving BER as low as 4.38×10^{-9}. Note that the WRC-FPLD injection-locked WRC-FPLD pair with partial coherence could also provide an OOK receiving power sensitivity of −25.5 dB at a BER of 10^{-9} and a 16-QAM OFDM transmission BER of 5.9×10^{-3}, which is considered as the most cost-effective master source to concurrently support multi-channel wavelength injection-locking when comparing with other candidates.

6.3 Summary

The effect of master coherence on the OOK and 12.5-Gbit/s OFDM signal transmission of the injection-locked slave WRC-FPLD in a 100-GHz channelized DWDM-PON system has been investigated. Increasing the coherence of the master source improves the frequency response and suppresses the RIN of injection-locked WRC-FPLD. By changing the injection master from ASE to TSL, the RIN of the injection-locked WRC-FPLD can be decreased by at least 15 dB. The SNR of the OOK signal carried by the slave WRC-FPLD increases from 6.07 to 10.8 by enhancing the injection coherence from non-coherence to high coherence. Increasing the master coherence suppresses the on-level noise of the transmitted OOK data such that the SNR is enhanced more than ER. When comparing the 1.25- and 2.5-Gbit/s transmissions carried by the slave WRC-FPLD injection-locked with masters of different coherences, the receiving power penalty of 3 dB is observed by upgrading the bit rates from 1.25 to 2.5 Gbit/s. On the other hand, the BER of the 16-QAM OFDM data is significantly enhanced from 1.5×10^{-1} to

4.38×10^{-9} by increasing the master coherence. Although the use of QAM-OFDM data could enhance the spectral efficiency, the degradation of the transmission performance with decreasing the injection coherence is more significant than that using the OOK data format. The QAM-OFDM data reveals a stronger correlation with the enhanced master coherence than the OOK for the injection-locked WRC-FPLD. Therefore, the coherence of injection light source is more important for the OFDM than OOK signals carried by injection-locked WRC-FPLD. Although the highest coherence leads to the best transmission performance, the TSL injection-locked WRC-FPLD is inappropriate for a cost-effective DWDM-PON, whereas the partially coherent WRC-FPLD injection-locked WRC-FPLD pair with a favorable cost could be considered as a more practical transmitter for the DWDM-PON system.

References

1. S.-J. Park, C.-H. Lee, K.-T. Jeong, H.-J. Park, J.-G. Ahn, K.-H. Song, Fiber-to-the-home services based on wavelength-division-multiplexing passive optical network. J. Lightwave Technol. **22**(11), 2582–2591 (2004)
2. D. Gutierrez, W.-T. Shaw, F.-T. An, Y.-L. Hsueh, M. Rogge, G. Wong, L.G. Kazovsky, Next-generation optical access networks. J. Lightwave Technol. **25**(11), 3428–3442 (2007)
3. J. Wang, M.K. Haldar, L. Li, F.V.C. Mendis, Enhancement of modulation bandwidth of laser diodes by injection locking. IEEE Photon. Technol. Lett. **8**(1), 34–36 (1996)
4. A. Murakami, K. Kawashima, K. Atsuki, Cavity resonance shift and bandwidth enhancement in semiconductor lasers with strong light injection. IEEE J. Quantum Electron. **39**(10), 1196–1204 (2003)
5. H.-D. Kim, S.-G. Kang, C.-H. Lee, A low-cost WDM source with an ASE injected Fabry-Perot semiconductor laser. IEEE Photon. Technol. Lett. **12**(8), 1067–1069 (2000)
6. P. Healey, P. Townsend, C. Ford, L. Johnston, P. Townley, I. Lealman, L. Rivers, S. Perrin, R. Moore, Spectral slicing WDM-PON using wavelength-seeded reflective SOAs. Electron. Lett. **37**(19), 1181–1182 (2001)
7. W. Lee, M.-Y. Park, S.-H. Cho, J. Lee, C. Kim, G. Jeong, B.-W. Kim, Bidirectional WDM-PON based on gain-saturated reflective semiconductor optical amplifiers. IEEE Photon. Technol. Lett. **17**(11), 2460–2462 (2005)
8. Y.-H. Lin, C.-J. Lin, G.-C. Lin, G.-R. Lin, Saturated signal-to-noise ratio of up-stream WRC-FPLD transmitter injection-locked by down-stream data-erased ASE carrier. Opt. Express **19**(5), 4067–4075 (2011)
9. H. Takesue, T. Sugie, Wavelength channel data rewrite using saturated SOA modulator for WDM networks with centralized light sources. J. Lightw. Technol. **21**(11), 2546–2556 (2003)
10. G.-R. Lin, Y.-H. Lin, C.-J. Lin, Y.-C. Chi, G.-C. Lin, Reusing a data-erased ASE carrier in a weak-resonant-cavity laser diode for noise-suppressed error-free transmission. IEEE J. Quantum Electron. **47**, 676–685 (2011)
11. G.-R. Lin, Y.-H. Lin, C.-J. Lin, Y.-C. Chi, G.-C. Lin, Reusing a data-erased ASE carrier in a weak-resonant-cavity laser diode for noise-suppressed error-free transmission. IEEE J. Quantum Electron. **47**(5), 676–685 (2011)
12. G.-R. Lin, Y.-H. Lin, Y.-C. Chang, Theory and Experiments of a Mode-Beating Noise-Suppressed and Mutually Injection-Locked Fabry-Perot Laser Diode and Erbium-Doped Fiber Amplifier Link. IEEE J. Quantum Electron. **40**(8), 1014–1022 (2004)
13. K.-M. Choi, J.-S. Baik, C.-H. Lee, Broad-band light source using mutually injected Fabry-Pérot laser diodes for WDM-PON. IEEE Photon. Technol. Lett. **17**(12), 2529–2531 (2005)

14. Z. Xu, Y.-J. Wen, W.-D. Zhong, C.-J. Chae, X.-F. Cheng, Y. Wang, C. Lu, J. Shankar, High-speed WDM-PON using CW injection-locked Fabry-Pérot laser diodes. Opt. Express **15**(6):2953–2962 (2007)
15. G.-R. Lin, T.-K. Chen, Y.-H. Lin, G.-C. Lin, H.-L. Wang, A weak-resonant-cavity Fabry–Perot laser diode with injection-locking mode number-dependent transmission and noise performances. J. Lightw. Technol. **28**(9), 1349–1355 (2010)
16. T.A. Birks, D. Mogilevtsev, J.C. Knight, P.S.J. Russell, Dispersion compensation using single-material fibers. IEEE Photon. Technol. Lett. **11**(6), 674–676 (1999)
17. Y.-S. Liao, H.-C. Kuo, Y.-J. Chen, G.-R. Lin, Side-mode transmission diagnosis of a multichannel selectable injection-locked Fabry-Perot laser diode with anti-reflection coated front facet. Opt. Express **17**(6), 4859–4867 (2009)
18. X. Jin, S.-L. Chuang, Bandwidth enhancement of Fabry-Perot quantum-well lasers by injection-locking. Solid-State Electron. **50**(6), 1141–1149 (2006)
19. G.-R. Lin, H.-L. Wang, G.-C. Lin, Y.-H. Huang, Y.-H. Lin, T.-K. Cheng, Comparison on injection-locked fabry-perot laser diode with front-facet reflectivity of 1 % and 30 % for optical data transmission in WDM-PON system. J. Lightwave Technol. **27**(14), 2779–2785 (2009)
20. G.-R. Lin, T.-K. Chen, Y.-C. Chi, G.-C. Lin, H.-L. Wang, Y.-H. Lin, 200-GHz and 50-GHz AWG channelized linewidth dependent transmission of weak-resonant-cavity FPLD injection-locked by spectrally sliced ASE. Opt. Express **17**(20), 17739–17746 (2009)
21. H. Kim, H.-C. Ji, C.-H. Kim, Effects of intraband crosstalk on incoherent light using SOA-based noise suppression technique. IEEE Photon. Technol. Lett. **18**(14), 1542–1544 (2006)
22. A.D. McCoy, B.C. Thomsen, M. Ibsen, D.J. Richardson, Filtering effects in a spectrum-sliced WDM system using SOA-based noise reduction. IEEE Photon. Technol. Lett. **16**(2), 680–682 (2004)
23. Y.-H. Lin, G.-C. Lin, H.-L. Wang, Y.-C. Chi, G.-R. Lin, Compromised extinction and signal-to-noise ratios of weak-resonant-cavity laser diode transmitter injected by channelized and amplitude squeezed spontaneous-emission. Opt. Express **18**(5), 4457–4468 (2010)
24. H.-C. Ji, I. Yamashita, K.I. Kitayama, Cost-effective WDM-PON delivering up/down-stream data and broadcast services on a single wavelength using mutually injected FPLDs, in *Proceedings of optical fiber communication conference*, Paper OTuH2, Feb 2008
25. G.-R. Lin, Y.-S. Liao, Y.-C. Chi, H.-C. Kuo, G.-C. Lin, H.-L. Wang, Y.-J. Chen, Long-cavity Fabry-Perot laser amplifier transmitter with enhanced injection-locking bandwidth for WDM-PON application. J. Lightw. Technol. **28**(20), 2925–2932 (2010)
26. C.-L. Tseng, C.-K. Liu, J.-J. Jou, W.-Y. Lin, C.-W. Shih, S.-C. Lin, S.-L. Lee, G. Keiser, Bidirectional transmission using tunable fiber lasers and injection-locked Fabry–Pérot laser diodes for WDM access networks. IEEE Photon. Technol. Lett. **20**(20):794–796 (2008)
27. S.-Y. Lin, Y.-C. Chi, Z.-W. Liao, H.-L. Wang, G.-C. Lin, G.-R. Lin, WDM-PON transmission using WRC-FLDs with AR coating reflectance of 0.5 % and 1.2 %, in *Proceedings of OECC*, pp. 83–84, 2012
28. J. Armstrong, OFDM for optical communications. J. Lightw. Technol. **27**(3), 189–204 (2009)
29. A.J. Lowery, Fiber nonlinearity pre- and post-compensation for long-haul optical links using OFDM. Opt. Express **15**(20), 12965–12970 (2007)
30. J.-M. Tang, P.-M. Lane, K.-A. Shore, High-speed transmission of adaptively modulated optical OFDM signals over multimode fibers using directly modulated DFBs. J. Lightw. Technol. **24**(1), 429–441 (2006)
31. X.Q. Jin, R.P. Giddings, E. Hugues-Salas, J.M. Tang, Real-time demonstration of 128-QAM-encoded optical OFDM transmission with a 5.25 bit/s/Hz spectral efficiency in simple IMDD systems uti-lizing directly modulated DFB lasers. Opt. Express **17**(22), 20484–20493 (2009)
32. E. Hugues-Salas, R.P. Giddings, X.-Q. Jin, J.-L. Wei, X. -Zheng, Y. Hong, C. Shu, M.-J. Tang, Real-time experimental demonstration of low-cost VCSEL intensity-modulated 11.25 Gb/s optical OFDM signal transmission over 25 km PON systems. Opt. Express **19**(4), 2979–2988 (2011)
33. A. Schimpf, D. Bucci, B. Cabon, Optimum biasing of VCSEL diodes for all-optical up-conversion of OFDM signals. J. Lightw. Technol. **27**(16), 3484–3489 (2009)

34. Y.-C. Chi, Y.-C. Li, H.-Y. Wang, P.-C. Peng, H.-H. Lu, G.-R. Lin, Optical 16-QAM-52-OFDM transmission at 4 Gbit/s by directly modulating a coherently injection-locked colorless laser diode. Opt. Express **20**(18), 20071–20077 (2012)
35. R.P. Giddings, E. Hugues-Salas, X.-Q. Jin, J.-L. Wei, J.-M. Tang, Experimental demonstration of real-time optical OFDM transmission at 7.5 Gb/s Over 25-km SSMF using a 1-GHz RSOA. IEEE Photon. Technol. Lett. **22**(11), 745–747 (2010)
36. T. Duong, N. Genay, P. Chanclou, B. Charbonnier, A. Pizzinat, R. Brenot, Experimental demonstration of 10 Gbit/s upstream transmission by remote modulation of 1 GHz RSOA using adaptively modulated optical OFDM for WDM-PON single fiber architecture, in *Proceedings of European conference on optical communication*, Paper Th.3.F.1, Sep 2008
37. G.-R. Lin, Y.-C. Chi, Y.-C. Li, J. Chen, Using a L-band weak-resonant-cavity FPLD for subcarrier amplitude pre-leveled 16-QAM-OFDM transmission at 20 Gbit/s. J. Lightwave Technol. **31**(7), 1079–1087 (2013)
38. K.-Y. Park, S.-G. Mun, K.-M. Choi, C.-H. Lee, A theoretical model of a wavelength-locked Fabry-Pérot laser diode to the externally injected narrow-band ASE. IEEE Photon. Technol. Lett. **17**(9), 1797–1799 (2005)